J Mater Sci (2011) 46:7319–7327
DOI 10.1007/s10853-011-5693-3

Effect of Sn addition on microstructure and dry sliding wear behaviors of hypereutectic aluminum–silicon alloy A390

X. F. Wu · G. A. Zhang

Received: 19 February 2011 / Accepted: 4 June 2011 / Published online: 16 June 2011

Abstract In this study, the effect of Sn addition on the microstructure and dry sliding wear behaviors of as-cast and heat-treated hypereutectic A390 alloys was investigated. The microstructural features of the alloys were characterized by means of optical microscope, scanning electron microscope (SEM), and energy dispersive X-ray spectroscopy techniques and their wear characteristics were evaluated at different loads. The worn morphologies of the wear surface were examined by SEM. The results show that the β-Sn in as-cast A390 alloy precipitates mainly in the form of particles within the Al_2Cu network on the interface of the eutectic silicon and α-Al phases and the grain boundaries of α-Al phase. The addition of Sn promotes the disintegrating and spheroidizing of both the eutectic and primary silicon of the A390 alloy during solid solution-aging treatment and β-Sn phase grains coalesces and grows, and some of them form the structure of Sn wrapping Si. The wear rates and friction factors of the as-cast and heat-treated A390 alloys with Sn are lower than those without Sn. At lower load, the addition of Sn changes the wear mechanism of as-cast A390 alloy from the combination of abrasive and adhesive wear without Sn into a single mild abrasion wear with Sn; at higher load, the wear of as-cast A390 alloy without Sn includes abrasion, adhesive, and fatigue one, while the addition of Sn effectively restrains the net-like cracks on the worn surface of the alloy and avoids the fatigue wear emerged.

X. F. Wu (✉) · G. A. Zhang
School of Materials Science and Engineering, Liaoning University of Technology, 169 Shiying Street, Jinzhou 121001, People's Republic of China
e-mail: hgd901@126.com

Introduction

The attractive properties of hypereutectic Al–Si alloys, e.g., low specific gravity, high strength at elevated temperature, excellent wear resistance, and low coefficient of thermal expansion make them attractive candidate materials for automotive, aerospace, and electronics applications, in particular in the applications where the alloys are a substitute for cast iron when the engineering advantage of light weight and wear resistance in service are considerations such as for the production of engine blocks, air compressor cylinders and cylinder heads [1–4]. However, the primary Si particles formed in the hypereutectic Al–Si alloys produced by casting methods, even though modified to refine them, are larger, and the Si particles themselves are hard and brittle, which causes the serious disseverance to the matrix and stress concentration at the tips or edges of the primary Si particles, leading to the cracking at the grain boundary or in primary silicon particles oneself, thereby, the mechanical properties, especially the elongation are significantly reduced [5]. On the other hand, a large number of hard primary silicon particles with sharp angles greatly aggravate machining performance, surface roughness increases, and as the primary silicon breaks away from the soft matrix very easily, abrasive wear and seizure between friction metals occur due to surface temperature rising [6, 7], which makes wearing capacity not be able to fully play and restricts the use of hypereutectic Al–Si alloys. In addition, when the alloys are used as parts such as friction pair, they are subject to surface-treatment, such as anodizing or Sn plating to reduce friction coefficient and improve abrasion resistance [8]. This increase the procedure and production cost, and the effective life of the parts is short due to the thinner coating. So it is an expecting object to provide a hypereutectic Al–Si alloy, which is excellent in free-machinability and abrasion resistance and maintains high strength.

It is known that adding an or some elements with low melting point for forming additional soft phases in a relatively hard matrix material (aluminum or copper) can provide self-lubricating properties to parts and improve the machinability and abrasion resistance of the material because of the resulting smooth surfaces, lower cutting forces, limited tool wear, and more easily breakable chips [9]. Tin (Sn) is an element with low melting point (220 °C) and exists in Al alloys in the forms of simple substance because of the solid insolubility between Sn and Al. Thus, the addition of Sn to Al alloys is capable of meeting many of the described requirements as well as acting as a solid lubricant to minimize the chances of seizure, which applied to bearings made of Al–Sn alloy [10]. The effects of Sn additions on the microstructure and properties of hypoeutectic and eutectic Al–Si alloys have been investigated by some researchers. Mohamed et al. [11] investigated the effect of trace additions of Sn on the mechanical properties of B319.2 and A356.2 alloys. Their results show that Sn-containing alloys have the higher ductility in the as-cast condition, while the mechanical properties of the heat-treated alloys decrease with increasing Sn content. They also reported that Sn and In combined provide better mechanical properties for Al–10.8Si–2.25Cu–0.3Mg in as-cast and aged conditions than may be obtained through the addition of Sn alone [12]. Kliauga et al. [13] found that the addition of 0.5 wt% Sn to Al–7Si–0.3Mg alloys (356 and A356) led to a reduction of the iron rich intermetallics volume fraction, and of hardness; Røset et al. [14] added 0.28 and 1 wt% Sn to a 6082 alloy with the intent of increasing its machinability without interfering in its extrudability; Recently, M. Anil et al. [15] studied the influence of tin content on tribological characteristics of spray formed Al–Si alloys and found a considerable increase in the wear resistance of Sn-bearing Al–12.5Si alloy with Sn addition. In addition, there is much information about the accelerating effect of trace Sn on precipitation hardening and increasing on the mechanical properties of hypoeutectic and eutectic Al–Si–Cu, Al–Si–Mg, or Al–Si–Cu–Mg alloys during solid solution-aging heat treatment [13, 14, 16].

But very limited information is available regarding the effects of Sn addition on the microstructure and dry sliding wear behaviors of the hypereutectic Al–Si alloys. Therefore, in this study, an attempt was made to reveal the dry sliding wear behaviors of hypereutectic aluminum–silicon alloy A390 with different amounts of Sn based on research of the microstructures of the alloys.

Experimental procedure

The chemical composition of the test alloys is presented in Table 1. Pure aluminum ingot and part of pure silicon block were charged into a graphite crucible and heated in using an electric resistance furnace. Then Al–Cu alloy and the remaining silicon block were added into the melt till they were completely melted. After that, pure magnesium was added into the melt with a bell jar. Then the melt was degassed with Hexachloroethane, and the modifying treatment was carried out with the addition of Al–2.5P master alloy and pure metal Sn with different amounts was added in the modified melt at 850 °C. Last, the melt was gently stirred and cast into a steel mold preheated at 200 °C to produce rods with 30 mm diameter. After casting, samples were solution heat treated at 480 °C for 8 h, quenched into warm (70 °C) water and then aged to a T6 condition at 195 °C for 8 h. The samples were mechanically ground, and then polished through standard routines. Each cross-section was etched using 0.5 vol.% hydrofluoric acid water solution. The microstructure and worn surface morphology of the alloys were investigated by an optical microscope and a scanning electron microscope (SEM) equipped with energy dispersive X-ray spectroscopy (EDS).

The hardness was measured using a Brinell hardness tester, and the magnitude of load was 9800 N with a 30 s load time. The hardness values were taken from the average of six measurements. In order to evaluate the effect of tin addition on the dry sliding wear behaviors of the A390 alloy, dry sliding abrasive wear tests were performed using a pin-on disk machine under loads ranging from 40 to 180 N. A bearing steel ring was employed as the counterface. Before and after the test, the pin was cleaned with ethanol and weighed. The wear rate was calculated from the results of the weight loss and sliding distance.

Results and discussion

Microstructures, hardness, and tensile properties

Figure 1 presents the optical microstructures of the as-cast and heat-treated A390 alloys without Sn and with 3%Sn modified by Al–2.5P master alloy. The as-cast A390 alloy without Sn modified by P consists of fine polyhedral or

Table 1 Chemical composition of Al–Si–Cu–Mg alloy

Elements	Si	Fe	Cu	Mn	Mg	Zn
Percentage/wt%	16.0–18.0	<0.5	4.0–5.0	<0.2	0.45–0.65	<0.1

blocky primary silicon phase distributed unevenly in a matrix that comprises dendritic α-Al grains and needle-like eutectic Si particles (Fig. 1a). After adding 3%Sn, the primary and eutectic silicon phase became slightly coarse, but the shape did not change (Fig. 1b). For the heat-treated A390 alloys without Sn modified by P, some eutectic silicon grains were changed from long needle-like shape in as-cast to thick short strip shape during heat treatment and the morphology of the primary silicon was not changed by heat treatment as shown in Fig. 1c. However, with the addition of 3%Sn, not only the eutectic silicon but also the primary silicon were disintegrated and spheroidized and many sharp angles of polyhedral or blocky primary Si disappeared and most of them became spherical as shown in Fig. 1d. This indicates that the addition of Sn promotes the spheroidizing of the eutectic and the primary silicon of the A390 alloy.

Back scattered electron image and its corresponding EDS analysis results of the as-cast and heat-treated A390 alloys with 3%Sn were shown in Fig. 2 and Table 2, respectively. It is visible that the white phases in the matrix with the mole fraction Sn of more than 98% (point A) are β-Sn, the gray white parts with the close to 2 mol ratio of Al/Cu (point B) are Al_2Cu. In the microstructure of the as-cast A390 alloy, β-Sn in the alloy is mainly in the form of particles within the Al_2Cu network, attached to the Si particles distributed on the interface of the eutectic silicon and α-Al phases and the grain boundaries of α-Al phase (Fig. 2a), which could also be seen in hypoeutectic Al–7Si–3Cu–0.3Mg with 0.17%Sn [12]. The distribution of the β-Sn phase is not uniform, but more uniform than that in hypoeutectic Al–7Si–3Cu–0.3Mg [12] due to the precipitation of the more silicon grains. After solid solution-aging treatment, many Sn particles within the Al_2Cu network, fine strip, and small block gather and merge around the spheroidized primary and eutectic Si phases, and some of them form the structure of Sn wrapping Si (Fig. 2b), which is consistent with the results on the microstructures of Al–Sn–Si alloys reported by Yuan et al. [17]. The 'peritectic-type' islands microstructure of hard phases surrounded with soft phases is the most advantageous to antifriction and wear resistance [17].

Previous studies have revealed that the heat treatment leads to significant changes for the eutectic silicon in the microstructure for hypereutectic alloys. After the heat treatment, the silicon present in the alloys gets spheroidized while the morphology of polyhedral shape primary silicon particles is not affected [18–20]. This experiment documents that the addition of Sn can change the morphology and size of both primary and eutectic silicon simultaneously (Fig. 2). Although the eutectic silicon in the microstructure for hypereutectic alloys without Sn got spheroidized in many heat treatment condition [18, 20], it did not in our experiment condition while with Sn did, indicating that the addition of Sn promotes the disintegrating and spheroidizing of the eutectic silicon in the

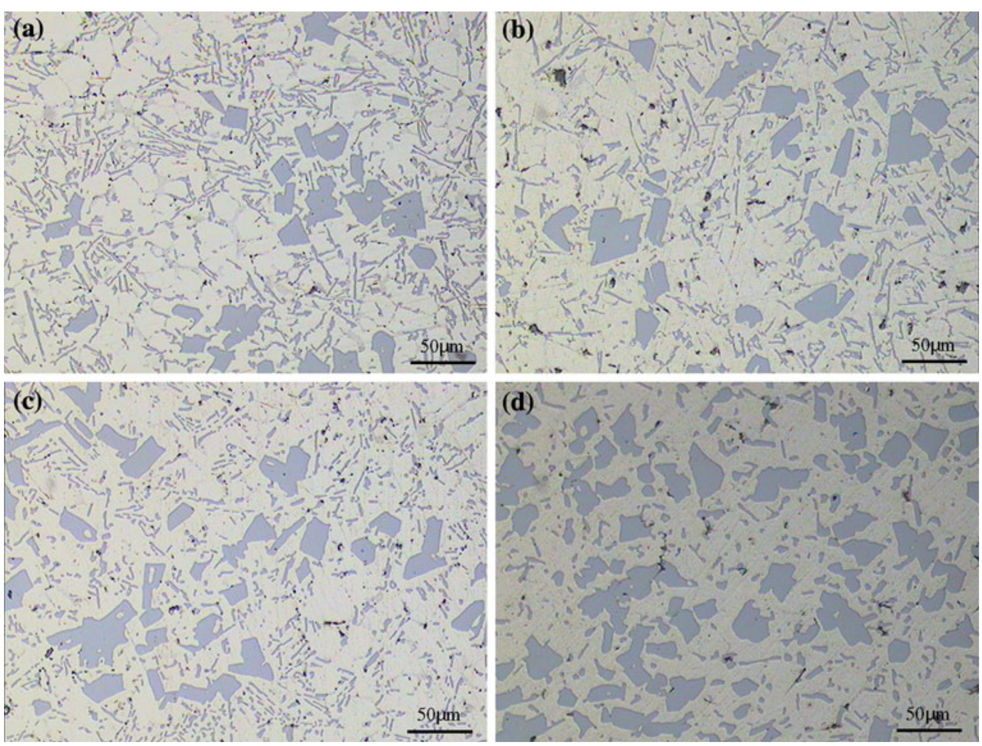

Fig. 1 Optical microstructures of A390 alloys in: **a** as-cast, 0%Sn; **b** as-cast, 3%Sn; **c** heat treated, 0%Sn; **d** heat treated, 3%Sn

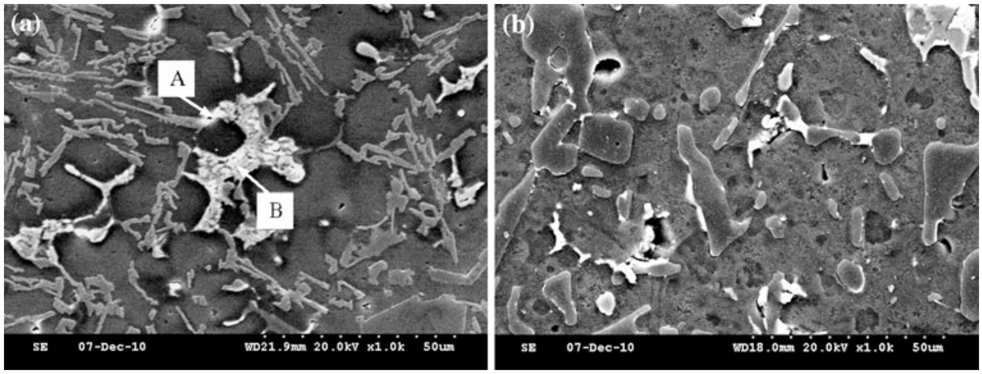

Fig. 2 SEM micrograph of A390 alloy in: **a** as-cast, 3%Sn; **b** heat treated, 3%Sn

Table 2 EDS analysis results of as-cast A390 alloy with 3%Sn in Fig. 2 (molar fraction, %)

Element	Point A	Point B
Al	0.57	61.79
Si	0.16	3.48
Cu	0.74	34.08
Mg	–	–
Sn	98.53	0.65

A390 alloy during the heat treatment. Diffusion plays an important role in the solutionizing of the alloys and microstructure changes, which is largely governed by the solutionizing temperature and the characteristic of the solute components in the alloys. Sn phase with low melting point melted into liquid around solid primary and eutectic silicon grains at 480 °C (the solutionizing temperature of this experiment), promoting the diffusion rate of Si atoms and therefore, Si atoms on the sharp angles of the primary and eutectic silicon grains are dissolved easily in Sn liquid or aluminum matrix, lending to the disintegrating and spheroidizing of the Si phases.

The influence of Sn addition level on the Brinell hardness of the as-cast and heat-treated alloys is shown in Fig. 3. It is seen that the influence trend of Sn addition level on the Brinell hardness of the as-cast and heat-treated alloys was found to be the same under all conditions, i.e., the Brinell hardness values decrease with Sn addition and the increase of Sn content. Typical hardness values of the alloy in the as-cast and heat-treated conditions were 104 and 137 HB, respectively. As 1.0%Sn was added to the as-cast alloys, the hardness values decreased to 89 and 126 HB, respectively. With increasing Sn content to 3%, the hardness values decrease slightly. However, when Sn content reach 5%, the hardness decreases sharply.

The lower hardness of the alloys with Sn may be ascribed to the formation of the soft β-Sn phase. It is worth noting that the Brinell hardness values of the heat-treated A390 alloys (both for the A390 alloys without Sn and with Sn) are significantly higher than those of the as-cast A390 alloys (both for the A390 alloys without Sn and with Sn) and the rate of decrease of the hardness values for the heat-treated alloys is lower than that for the as-cast alloys with increasing Sn content. High hardness for the heat-treated alloys is mainly due to the effect of solution and aging treatment on the matrix which precipitated phase GP area (mainly for GP II area) and the metastable phase (θ', β') obtained through the treatment, lending to the effectively improvement of the hardness of the A390 alloys. The Sn solubility in pure Al is 0.03 wt% and this would be enough for interfering in the precipitation behavior, by trapping vacancies [13]; on the other hand, small Sn precipitates in the Al matrix have already been observed in rapid solidified or quenched Al–Si–Mg–Sn alloys [21], and both events could act to enhance the number of nucleation sites for the precipitates and hardening rate, which is the main reason for the lower rate of decrease of the hardness values for the heat-treated alloys with Sn compared with the as-

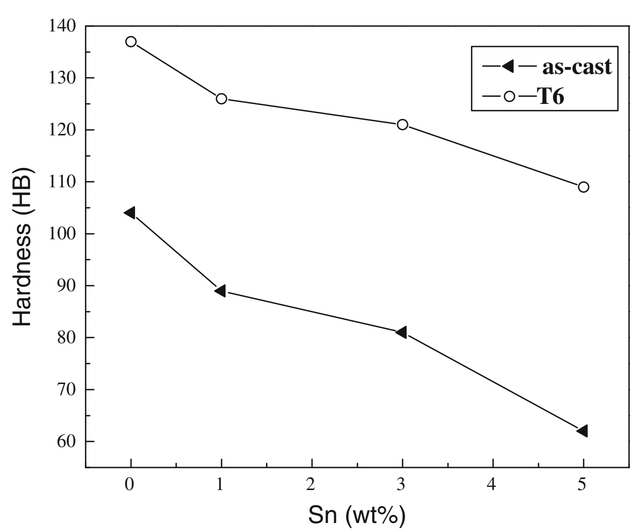

Fig. 3 The curves of hardness values vary with the contents of Sn

cast alloys with Sn with increasing Sn content. The above results also prove that Sn addition had little negative impact on Cu and Mg precipitation hardening during aging.

Variations of tensile properties with Sn content for the as-cast and heat-treated alloys are shown in Fig. 4. It is clear that the trend of variations in the ultimate tensile strength of the as-cast alloys with Sn content was corresponded to that of variations in hardness values, i.e., the UTS of Sn-containing alloys decreased with an increase in Sn content and were lower as compared to Sn-free alloys. Typical UTS value of the as-cast alloy was 241 PMa and was reduced by 6.6, 23.7, and 31.1% with an increase in Sn content from 1, 3 to 5%Sn, respectively. Lower strength properties for the alloys with Sn are attributed to the distribution of soft Sn, mainly on the phase interface of the eutectic silicon and α-Al phases or the grain boundaries of α-Al phases. The elongation of the as-cast alloy first increased, and then decreased with an increase in Sn content. However, for heat-treated alloys, the UTS values increased slightly with an increase in Sn content from 0 to 1%, and then diminished slightly. The variations of elongation with Sn content were similar to UTS ones.

Wear rates and friction factors

Figure 5 shows the effects of Sn contents on the wear rates and friction factors for the investigated as-cast and heat-treated A390 alloys under the load of 40 N. The wear rates decreased with Sn content at first, reached a minimum at 3%Sn, and then increased with increasing of Sn (Fig. 5a), but were not larger than those of the Sn-free alloys. The relationships of the friction factors with Sn content are similar to those of the wear rates with Sn content (Fig. 5b).

Figure 6 displays the variation in the wear rates of the alloys with applied loads. Obviously, the wear rates of the alloys increased with increasing load. Furthermore, it can be clearly observed that the wear rates of the as-cast alloy

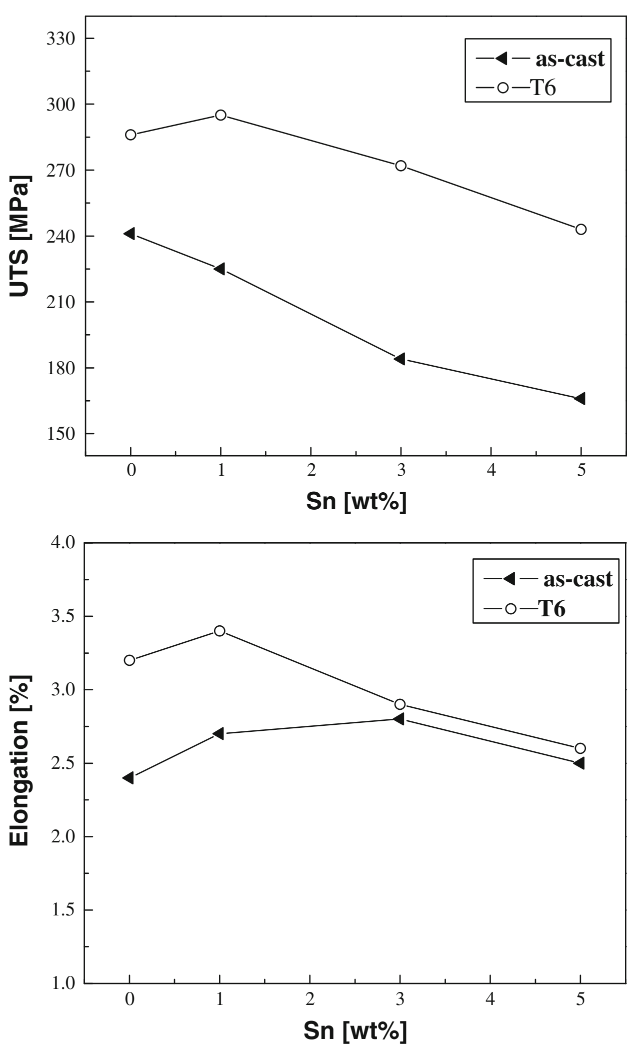

Fig. 4 The curves of tensile properties vary with the contents of Sn

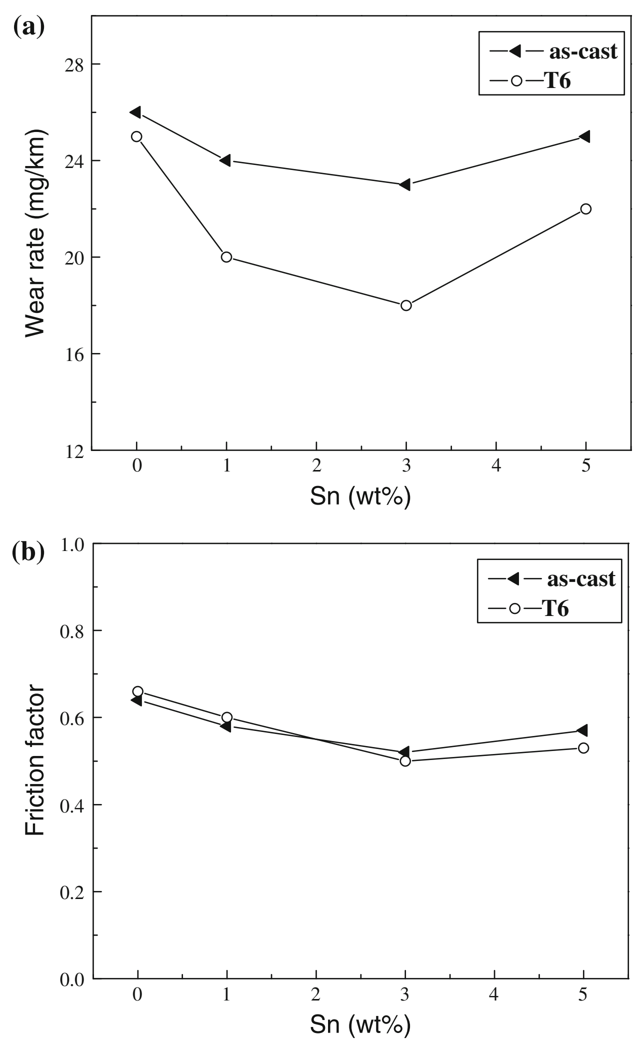

Fig. 5 The curves of **a** wear rates and **b** friction factors vary with the contents of Sn

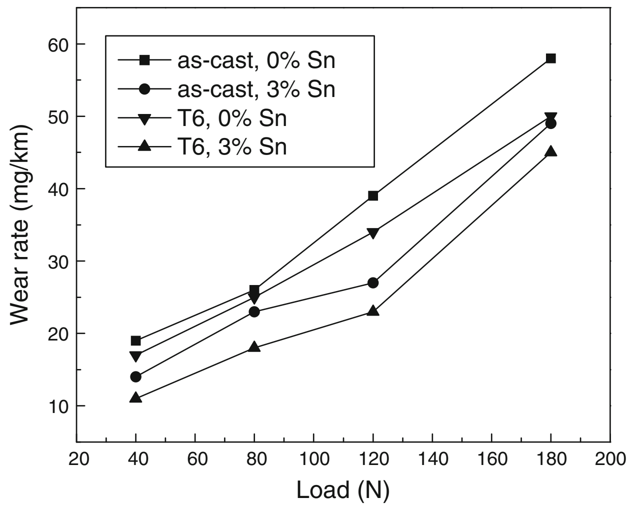

Fig. 6 The curves of wear rates vary with load

with Sn are lower than those of the as-cast alloy without Sn in the entire applied load range, especially under the load of about 120 N. In addition, the wear rates of the heat-treated A390 alloys (both for the A390 alloys without Sn and with Sn) are lower than those of the as-cast A390 alloys (both for the A390 alloys without Sn and with Sn), respectively. Furthermore, the heat-treated alloy with Sn still displayed a lower wear rate and superior wear resistance compared with the heat-treated alloy without Sn. Therefore, it can be concluded that both the addition of Sn and heat treatment are beneficial to improve the wear resistance of A390 alloys. Above results also indicate that the wear rates of all the investigated A390 alloys are proportional to the hardness, which not is the same as the results obtained in soft particles-free materials. Thus, the wear rate and mechanism for the materials containing soft particle phases may also does not totally depend upon the hardness of the materials.

The low wear rate for the alloys with Sn is mainly due to the self-lubrication function of β-Sn phase in the friction process. The effect of soft phase and their content on wear and frictional behavior of materials have been investigated and the improvement of the wear resistance for many Al alloys by adding soft Pb, graphite, Bi, and Sn have been demonstrated by many investigators [11, 15, 22–25]. For the A390 alloys with Sn, the soft Sn acts as an extreme pressure lubricant and is smeared over the sliding surface by forming a thin film of low shear strength between the mating surfaces during dry sliding, and in turn reduces the contact area between the specimen and the counterface and leads to easy shearing during sliding between two surfaces and thus insures a low frictional forces [15, 25]. In the process of sliding, the applied pressure was born by the underlying Al–Si alloy matrix, whereas, shearing takes place in a thin film of Sn having low shear strength. The structure of soft Sn combined with hard Si in the A390 alloys with Sn (Fig. 2) and the characteristic of the increasingly softening of Sn with low melting point with increasing surface temperature during the dry sliding insure a better smearing to avoid metal–metal contact during sliding, resulting in the decreases of the wear rates of the alloys with Sn. In addition, for the heat-treated A390 alloys, the addition of Sn still promotes the spheroidizing of both the eutectic and the primary silicon in the alloys (Figs. 1, 2) and precipitation hardening (Fig. 3) during the heat treatment, which facilitates the improvement on the wear resistance of the alloys. The investigations of hypereutectic Al–Si alloys showed that their mechanical properties are mainly determined by some metallurgical factors such as [26, 27]: (1) the morphology, size, and distribution of the primary and eutectic silicon crystal particles; (2) the cohesion between the silicon crystal particles and the matrix; and (3) the ease with which the particles crack. Spheroidized silicon crystals can considerably relieve the localized stress concentration at spheroidized silicon/α-aluminum interface. During the dry sliding process, the spheroidized silicon phase in the Al–Si alloys would effectively retard the crack nucleation and propagation propensities at the interface. Moreover, the excellent bonding between spheroidized silicon crystals and Al matrix may further increase the wear resistance of the alloys.

Worn surface and mechanism

In order to reveal the wear behavior and mechanism, the worn surfaces of as-cast without Sn, as-cast with Sn, heat treated without Sn, and with Sn A390 alloys were examined under SEM. Figure 7 shows SEM micrographs of worn surfaces of the alloys, tested at low load of 40 N. It can be seen that the worn surface of as-cast A390 alloy without Sn appeared deep and wide plowing grooves parallel to the motion direction of which their maximum width reached 15 μm and a lot of dimples and local adherent scars could also be seen in the surface, as shown in Fig. 7a, which demonstrates that abrasive and adhesive wear appear to be the main wear mechanism of the alloys. With 3%Sn adding, a small number of shallow and narrow grooves only occurred, which is a single mild abrasion wear (Fig. 7b). After heat treated, the worn surface grooves of the A390 alloy without Sn became shallow and narrow and there were a small amount of small cavities (Fig. 7c), while the worn surface of the alloy with Sn had a rather smooth appearance as a result of homogeneous wear and the grooves became more shallow and narrower (Fig. 7d).

Figure 8 shows SEM micrographs of worn surfaces of the alloys, tested at high load of 180 N. Compared with the worn surface of as-cast A390 alloy without Sn at low load

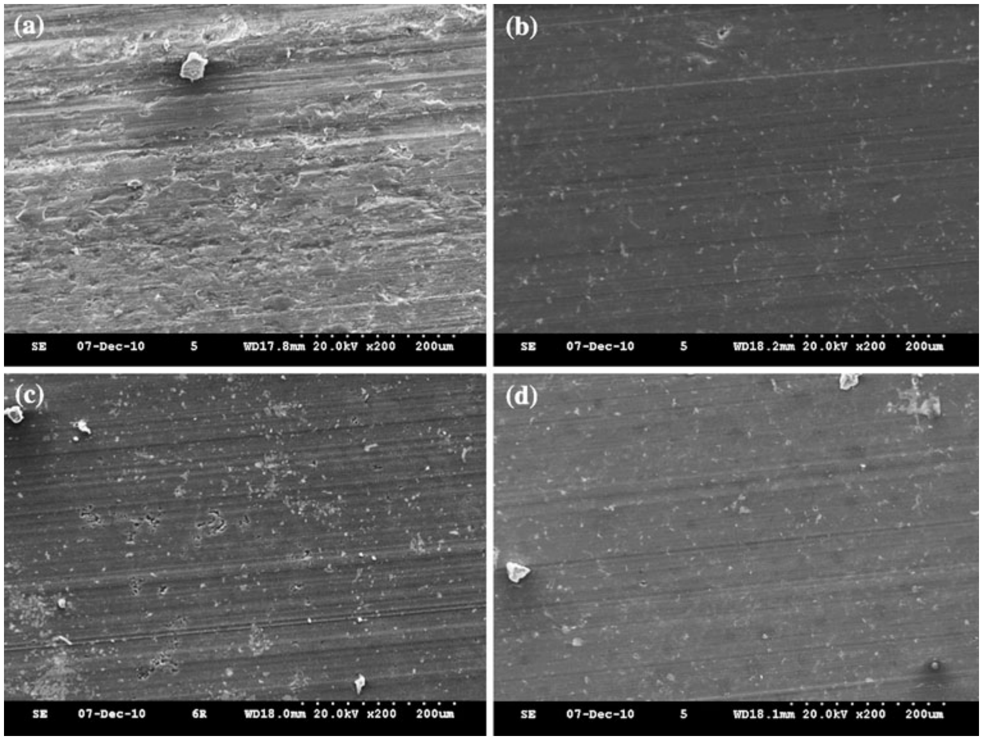

Fig. 7 SEM micrographs of worn surfaces of the A390 alloys under 40 N load in: **a** as-cast, 0%Sn; **b** as-cast, 3%Sn; **c** heat treated, 0%Sn; **d** heat treated, 3%Sn

of 40 N, the one at high load of 180 N appeared deeper and wider grooves of which their maximum width reached 25 μm and dimples and local adherent scars were increased in the surface, and a lot of net-like cracks were also produced, the small pieces around the cracks and the matrix are in felled out state, some had been delaminated and separated from the surface, this is a combination of abrasion wear, adhesive wear and fatigue wear, as shown in Fig. 8a. After 3%Sn adding, the net-like cracks disappeared, only grooves, dimples local, and adherent scars were left, these grooves are just wider and deeper than those at low load conditions, and the worn surfaces exhibited great plastic deformation. So a single abrasion wear at low load conditions was changed into the combination of abrasion wear and adhesive wear (Fig. 8b). The worn surface of heat-treated alloy without Sn appeared also no net-like cracks, but deep and wide grooves and dimples, across which were numerous cavities (Fig. 8c). With Sn adding, the heat-treated alloy had a worn surface only with grooves, but compared with that at low load conditions, the grooves were deeper and wider (Fig. 8d).

Wear process generally experiences three stages, i.e., surface interaction, surface damage, and wearing pull-out, and wear forms mainly include abrasion wear, adhesive wear, fatigue wear, and chemical wear, etc. In the wear process of the hypereutectic Al–Si alloy such as A390 alloy, primary and eutectic Si particles with high hardness provide supporting and protection for relatively soft aluminum matrix. These Si particles are easy to cause the plastic deformation of the contact part of the Al–Si alloy and counterpart, leading to the presence of dimples with different depths and widths. Meanwhile, the parts around the dimples on the counterpart are squeezed and piled up, resulting in the softer matrix of the Al–Si alloy being squeezed. After the extrusion process and the plastic deformation caused are repeated several times, cracks are initiated easily within Si phase particles or the contact part of the Si particles and the aluminum matrix, and propagated gradually into the interior of the Si particles under the repeated impact of the load, eventually leading to fracturing and dropping of the Si particles in the alloys. These dropping hard Si particles make relative motion along the friction direction on the soft aluminum matrix under the act of inertial force, causing the secondary cutting of the matrix, thus forming plows with different depths and widths.

The wear surfaces of the A390 alloys without Sn, whether at a low load (Fig. 7a) or a high load (Fig. 8a), appear lots of dimples and local adherent scars except deeper and wider plows, namely abrasion wear and adhesive wear are happened simultaneously in the friction process. Adhesion wear may be caused due to the absence of self-lubricating properties of the A390 alloy, thus the local surface is easily teared and adhered to the counterpart

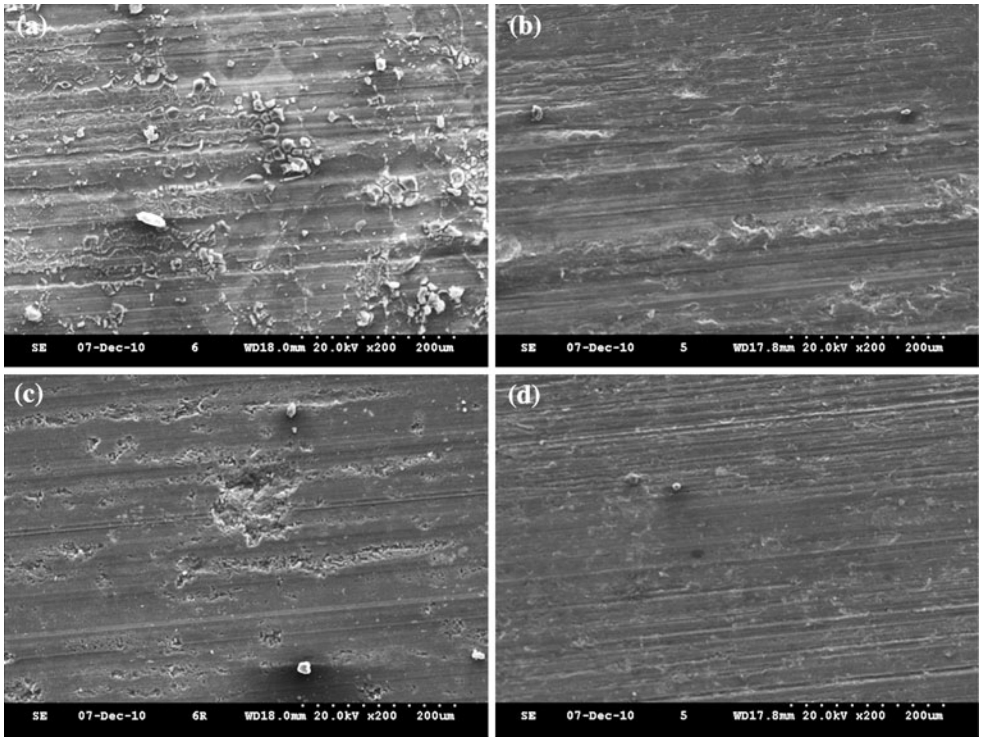

Fig. 8 SEM micrographs of worn surfaces of the A390 alloys under 180 N load in: **a** as-cast, 0%Sn; **b** as-cast, 3%Sn; **c** heat treated, 0%Sn; **d** heat treated, 3%Sn

under the act of a load. There are still a large number of net-like cracks and delamination under high load (Fig. 8a). This is attributed to the fact that cyclic stress produced during the dry sliding causes the surface fatigue wear and crack source is formed on surface or sub-surface, then, the fatigue cracks are propagated, causing the surface dropping. After 3%Sn is added, soft β-Sn phase with low melting point is formed and displays self-lubrication function in the friction process, making the alloy surface form oil film with strong toughness and avoiding tearing the A390 alloy surface and the appearing of adhesion wear under low load conditions. Meanwhile, in high load conditions, the microstructure of as-cast alloy with Sn (Fig. 8b) protects the Si phase, constrains the propagation of surface cracks and avoids the A390 alloy that occurs fatigue wear. As the precipitated phase GP area (mainly for GP II area) and the metastable phase (θ', β') obtained through solution and aging treatment can effectively improve the hardness of A390 alloy, after solution and aging treatment, whether the alloy without or with Sn, their wear-resisting properties are improved.

Conclusions

The effects of Sn addition on the microstructures and dry sliding wear behaviors of hypereutectic A390 alloys were investigated. The following conclusions can be drawn:

(1) Adding Sn to as-cast hypereutectic A390 alloys only slightly change the microstructure of the alloys, while promoting the disintegrating and spheroidizing of both the eutectic and the primary silicon of the A390 alloy during solid solution-aging treatment.

(2) β-Sn in as-cast A390 alloy precipitates mainly in the form of particles within the Al_2Cu network, attached to the Si particles distributed on the interface of the eutectic silicon and α-Al phases and the grain boundaries of α-Al phase; during heat treatment, β-Sn phase coalesces and grows and some of them form the structure of Sn wrapping Si.

(3) The wear rates and friction factors of the as-cast and heat-treated A390 alloys with Sn are lower than those without Sn and decrease at first, reach a minimum at 3%Sn, then increase with the increase of Sn content.

(4) The heat-treated alloys (both for the A390 alloys without Sn and with Sn) displayed a lower wear rate and superior wear resistance compared with those of the as-cast alloys.

(5) At lower load, the addition of Sn change the wear mechanism of as-cast A390 alloy from the combination of abrasive and adhesive wear without Sn into a single mild abrasion wear with Sn.

(6) At higher load, the wear mechanism of as-cast A390 alloy without Sn includes abrasion, adhesive, and fatigue wear, while the addition of Sn effectively

restrains the net-like cracks on the worn surface of the alloy and avoids the fatigue wear emerged.

References

1. Clegg AJ, Das AA (1977) Wear 43:367
2. Gupta M, Ling S (1999) J Alloys Compd 287:284
3. Prasad BK, Venkateswarlu K, Modi OP, Yegneswaran AH (1996) J Mater Sci Lett 15:1773
4. Davis FA, Eyre TS (1994) Tribol Int 27:171
5. Dwivedi DK (2006) Mater Design 27:610
6. Dey SK, Perry TA, Alpas AT (2009) Wear 267:515
7. Dwivedi DK (2004) Mater Sci Eng A 382:328
8. Ammar IA, Darwish S, Khalil MW, El-Taher SA (1989) Mater Chem Phys 21:1
9. Torabin H, Pathak JP (1994) Wear 177:47
10. Schouwenaars R, Jacobo VH, Ortiz A (2007) Wear 263:727
11. Mohamed AMA, Samuel FH, Samuel AM, Doty HW, Valtierra S (2008) Metall Mater Trans A 39:490
12. Mohamed AMA, Samuel FH, Samuel AM, Doty HW (2009) Metall Mater Trans A 40:240
13. Kliauga AM, Vieira EA, Ferrante M (2008) Mater Sci Eng A 480:5
14. Røset J, Saeter JA, Ustad T, Reiso O (2002) Mater Sci Forum 396–402:1205
15. Anil M, Srivastava VC, Ghosh MK, Ojha SN (2010) Wear 268:1250
16. Silcock JM (2002) Scr Mater 46:389
17. Yuan GC, Li ZJ, Lou YX, Zhang XM (2000) Mater Sci Eng A 280:108
18. Ogris E, Wahlen A, Lüchinger H, Uggowitzer PJ (2002) J Light Met 2:263
19. Sharma R, Dwivedi DK (2005) Mater Sci Eng A 408:274
20. Xu CL, Yang YF, Wang HY, Jiang QC (2007) J Mater Sci 42:6331. doi:10.1007/s10853-006-1189-y
21. Kliauga AM, Ferrante M (2002) Mater Sci Eng A 337:67
22. Rudrakshi GB, Srivastava VC, Ojha SN (2007) Mater Sci Eng A 457:100
23. Al-Rubaie KS, Goldenstein H, De Mello JDB (1999) Wear 225–229:163
24. Muratoglu M, Aksoy M (2006) J Mater Process Technol 174:272
25. Srivastava VC, Rudrakshi GB, Uhlenwinkel V, Ojha SN (2009) J Mater Sci 44:2288. doi:10.1007/s10853-008-2924-3
26. Prasad BK, Venkateswarlu K, Modi OP, Yegneswaran AHJ (1996) Mater Sci Lett 15:1773
27. Haque MM, Sharif A (2001) J Mater Process Technol 118:69